

Original Article

Cost-benefit methodology for road slope stabilisation

Ellen B. Robson^{a,*}, David G. Milledge^b, Stefano Utili^b, Michael Bründl^{c,d}^a Institute of Hazard, Risk, and Resilience, Durham University, Durham, UK^b School of Engineering, Newcastle University, Newcastle upon Tyne, UK^c WSL Institute for Snow and Avalanche Research SLF, Davos Dorf, Switzerland^d Climate Change, Extremes and Natural Hazards in Alpine Regions Research Centre CERC, Davos Dorf, Switzerland

ARTICLE INFO

Keywords:

Slope stability

Cost-benefit analysis

Road slope stabilisation

Roads

Hillslope-storage Boussinesq

Cut slopes

ABSTRACT

Cost-benefit analyses are conducted to evaluate the cost efficiency of road slope stabilisation measures to aid road planning, design, maintenance, and repair. Most cost analyses are based on a statistical framework that requires a database of slope failures. However, databases can be costly to compile, and they tend to compare options that satisfy the same global factor of safety or partial factors of safety (e.g. EC-7) neglecting the fact that each measure reduces the risk of slope failure by a different extent. Here, we present a novel methodology to evaluate the cost efficiency of different road slope stabilisation measures based on direct costs and a rigorous but parsimonious mechanistic and probabilistic geotechnical slope stability assessment. Unlike other cost analyses for slope stability, our methodology accounts for uncertainty in slope geomaterial characteristics, as well as for hillslope hydrology. Probabilistic slope stability analyses accounting for the effect of time-varying slope seepage are performed using the CUTSTAB-P methodology to estimate the frequency of slope failure. The methodology is demonstrated on a cut slope in Nepal, assessing four different road slope stabilisation measures that are implemented in Nepal: (1) the cut slope with no additional support; (2) reprofiling to a shallower inclination; (3) a mortared masonry wall; and (4) an anchoring system. We find that an anchoring system is the most cost-efficient road slope stabilisation measure for this cut slope, and that a mortared masonry wall is least cost-efficient. This is despite the mortared masonry wall having much lower initial investment costs than the anchoring system. Mortared masonry walls are hugely common along roads in Nepal. We also make an approximation of indirect costs. With this addition, we find that the anchoring system remains the most cost-efficient method.

1. Introduction

The construction of roads in hilly and mountainous terrain often requires excavating many kilometers of cut slopes. These slopes often require stabilisation measures (including mechanical stabilisation, bioengineering techniques, earthwork techniques, and ground improvement techniques) to prevent failure. Installation techniques, materials employed, and cost of measures vary widely, with the stabilisation measure adopted being highly dependent on the cut slope characteristics (e.g. geology, geometry, and hydrology of the slope), as well as spatial extent of the cut slope, budget, and time constraints.

According to Hearn [14], 70 % of slope failures on mountain roads are shallow instabilities in cut slopes. Cut slope failures can pose an immediate risk to people and property during failure, and can block roads, damage structures, and destabilise adjacent slopes for months

after. Recovery involves clearing debris, re-excavating, and re-stabilising the cut slope. This is costly to the economy, livelihoods, and the environment; yet it is a situation that occurs every year during the 'wet season' on roads throughout hilly low and lower-middle income countries (LIC/LMIC) [26,14,37]. Studies to justify investment in road slope stabilisation suggest that an initially high investment is often more cost-efficient than a cycle of inaction, failure, and repair [36,32]. Cost analysis methodologies are common practice by consultancies for road slope stabilisation design in High Income Countries (HICs) although there is not a commonly accepted framework to do so and the level of model sophistication and assumptions adopted by consultants is highly variable [43]. In many LIC/LMICs cost-analysis methods/tools are less commonly applied to road construction projects [6,33]. This means that there is little understanding of what measures are most cost-efficient (achieving the desired stability with the least resources) over time and

* Corresponding author.

E-mail address: ellen.robson@durham.ac.uk (E.B. Robson).<https://doi.org/10.1016/j.trgeo.2024.101282>

Received 3 April 2024; Received in revised form 20 May 2024; Accepted 28 May 2024

Available online 3 June 2024

2214-3912/© 2024 The Author(s). Published by Elsevier Ltd. This is an open access article under the CC BY license (<http://creativecommons.org/licenses/by/4.0/>).

little means to justify longer-lasting measures [33]. This in turn might result in a mistaken preference for low-initial-cost solutions given humans' well-documented 'present bias' [7].

In road construction, as well as landslide and slope failure contexts, cost analyses generally take the form of a cost-benefit analysis (CBA) which assigns monetary values to both the benefits and the costs of an intervention to determine the economic efficiency of the intervention [21,11]. CBAs for slope failure generally account for direct costs (associated with direct damage, debris clearance, and slope remediation) and/or indirect costs (associated with the knock-on effects of failure). For example, the Federal Office for the Environment in Switzerland utilises an online CBA tool, EconoMe, which incorporates both direct and indirect costs, to plan mitigation projects for a number of hazards in Switzerland [3]. The tool is one of the most advanced in the CBA sector to the authors' knowledge. This tool is used to perform risk analyses based on intensity maps of the hazard incorporating scenarios with different return periods. The probability of the hazard occurring is predefined in the tool based on historic databases. The expected losses are calculated as a product of hazard and exposure before the mitigation and after the mitigation [3]. A similar approach, but for landslide costs to property, is outlined by AGS [44].

To conduct a CBA to evaluate mitigation/stabilisation measures, requires determining the probability/frequency of slope failure [19]. Current methods to do so can be categorised into: (1) statistical analysis of a landslide database [3,12,20,16]; and/or (2) mechanistic slope stability analysis accounting for uncertainty and spatial variability of the slope hydro-mechanical properties [23] and/or rainfall conditions [19]. While statistical models are still the most common method for road slopes, their predictive capability depends on the similarity of the slope analysed to the set of slopes on which the model has been trained, which is seldom the case. Statistical models require large training datasets so that information is available for the chosen stabilisation measures and a particular slope-storm combination can be modelled. Slope failure databases are expensive to compile and, therefore, are more likely to be available in HICs such as Hong Kong [47,28,1] or Germany [20]. In practice such abundant data are rare even in HICs; thus considerable interpolation is required across slope types, forcing conditions and stabilisation measures, introducing large approximations. Where data is sparse the problem is even more severe, for example: smaller scale (e.g. cut slope) slope failures that cannot be identified on satellite imagery [19], or in LIC/LMIC which are typically data-poor and/or lack the resources to collate the data. However, Laos is one exception where a rich landslide database [17] has been used to determine indirect and direct costs on the national road network, and to evaluate the economic justification for increased investment in stabilisation measures [16]. They develop a matrix to outline the levels of economically justifiable investment based on annual average daily traffic and a range of landslide frequencies. Prior to this work, there was no database of landslides along roads in Laos [15].

Note that CBA methodologies used to evaluate slope stabilisation/mitigation measures sometimes produce alternative measures of cost-efficiency to the typical ratio of benefits to costs produced in traditional CBA frameworks. These CBA methodologies attribute a monetary value to the cost of remediating the slope failure, as well as to the benefit of risk reduction (i.e. the slope not failing), which can be difficult to uncouple, especially in terms of direct costs. Thereby, often a single monetary value is given as a measure of the cost-efficiency for the slope stabilisation. In cases where indirect costs are considered, the indirect costs that are saved as a consequence of the slope not failing can be more easily defined as benefits [19].

Mechanistic methods provide a good alternative to statistical (database-driven) methods to estimate probability of failure where landslide observations are limited. They are powerful because they enable: (1) a site-specific comparison of alternative stabilisation measures with very precise user control over the specifics of the slope design; and (2) a comparison for the same forcing conditions. Both features are very

difficult to achieve within a statistical framework because of the necessarily large pool of training data required to estimate the probabilities associated with each stabilisation measure. Application of mechanistic approaches have been surprisingly rare. Holcombe et al. [19] used such an approach to demonstrate the value of mitigation measures to protect a village in St. Lucia from landslides. They modelled landslide hazard and vulnerability before and after the implementation of mitigation, and monetised direct and indirect benefits. Mitigation costs were estimated based on previous mitigation works nearby and the present value of expected landslide costs calculated accounting for the time value of capital (discount factor) and the probability that a landslide will occur in that year.

One of the primary limitations of employing mechanistic approaches is their sensitivity to site-specific ground strength and pore pressure characteristics that are often difficult to constrain, introducing considerable uncertainty in absolute estimates of slope failure probability. While Holcombe et al. [19] use a deterministic slope stability analysis, which does not account for ground material variability, probabilistic stability analyses can account for this uncertainty to some degree [23]. However fundamental limitations remain around parameter uncertainty and its impact on the absolute probability of failure. Reducing this uncertainty through measurements, as Holcombe et al. [19] does, requires costly and time-consuming field/laboratory work which is problematic if the approach is to be scaled up beyond single-site applications. It is important to note that since these uncertainties are primarily associated with parameters that are unaffected by the type of chosen stabilisation measures, their impact on the relative differences in probability of failure are far smaller than on absolute probability. Therefore, mechanistic approaches are particularly powerful for comparing the cost efficiency of different stabilisation measures for the same slope.

Geotechnical practitioners often compare stabilisation solutions that satisfy the same global or partial factors of safety (FoS), e.g. EC-7, and choose the cheapest option, implicitly assuming that solutions that satisfy the minimum requirement in terms of safety are equally good. But this is not the right way to determine the most cost-efficient option since the probability of failure (or survival) associated with solutions exhibiting similar or even the same FoS or overdesign ratio (for Eurocode 7 compliance) may be vastly different due to different levels of uncertainty associated with each solution [8]. To avoid this pitfall, the probability of failure itself needs to be considered in the evaluation of the best option. But, there is still a subjective element with regard to the importance attributed to risk reduction. For instance, consider two solutions both complying with the minimum safety requirement, should a cheaper one bringing less risk reduction be preferred to a more expensive one enabling a higher risk reduction?

In this paper we present the first methodology (to the authors' knowledge) for road cut slope CBA driven by mechanistic stability analyses. A CBA approach is used, monetising the efficiency of the stabilisation measure in terms of the direct costs to rectify slope failure, and thereby avoiding subjectivity. Using this method, the cost efficiency of different stabilisation measures can be determined, including a scenario with no stabilisation (a base case), and compared against one another. For each engineering measure considered, first, the associated frequency of failure over the entire lifetime of the cut slope is calculated, and second, the cost associated with each failure is determined. In this way the different levels of risk reduction are explicitly considered in the determination of the frequency of failure; and an objective criterion for the choice of the best solution (i.e. which is cheaper over the lifetime of the road) becomes available. The frequency of slope failure is estimated using a methodology recently proposed by Robson et al. [35], which combines probabilistic stability analyses with the hillslope-storage Boussinesq (HSB) model to determine the time-varying seepage induced by rainfall over the road lifetime. We name this method 'Probabilistic Cut Slope Stability Analysis' (CUTSTAB-P), and will refer to it as CUTSTAB-P herein. In the CUTSTAB-P method, both the uncertainty of ground properties and realistic time-varying phreatic surfaces

within the slope (accounting for the hillslope groundwater regime) are accounted for. We opted to utilise a mechanistic model because we believe the benefits of site-specific comparisons outweigh the aforementioned limitation of constraining absolute probability. Note that any method (either statistical or mechanistic) estimating the frequency of failure of a given cut slope subjected to a prescribed stabilisation scenario could equally be employed by the cost-benefit analysis methodology presented herein. The CBA methodology presented here provides an annual cost for each slope stabilisation measure evaluated, to achieve an objective comparison between measures and a clear rationale for the choice of the best. The methodology is demonstrated on a road cut slope in Nepal, to evaluate the cost-efficiency of four different slope stabilisation measures employed in Nepal.

2. Methodology

The framework for the CBA methodology is outlined in Section 2.1. The cost of rectifying slope failure is dependent on the annual frequency of slope failure (F_f) predicted over a period of time, and thus on the stabilisation measure implemented. The methodology employed to determine the F_f , CUTSTAB-P, is taken from Robson et al. [35] with a summary outlined in Section 2.2.

The methodology is demonstrated on a real road cut slope situated along the Narayanghat-Mugling road in Chitawan, Nepal. Details of the site and a background to road cut slopes in Nepal are outlined in Section 2.3. The costs are estimated using a region-specific system of rate attribution that provides standardised costing estimates for budgeting. These are applied to each stabilisation measure evaluated in Section 2.3.5.

2.1. Cost analysis framework

The outcome of this analysis is presented as a cost per annum (CE_n) for each stabilisation measure tested, which can be used to compare the cost efficiency of different stabilisation measures. The methodology focuses on direct costs since indirect costs are difficult to estimate and can be ambiguous. We use a series of equations adapted from Bründl, et al. [3] to determine the cost of the slope stabilisation measure per annum (CE_n). The values used in the case study to demonstrate this methodology are outlined in Section 2.3.5.

Firstly, the initial investment I_0 of the stabilisation measure is determined by:

$$I_0 = C(e) + C(s) + R_v(C(e) + C(s)) \quad (1)$$

where the cost of implementing the slope stabilisation measure is partitioned into the cost of earthworks $C(e)$ and of building a structure $C(s)$, and R_v is the country-specific value-added tax (13 % for Nepal in 2023). $C(e)$ can be estimated as the cost of excavation including the disposal of material (accounting for the geometry and type of material to be excavated). $C(s)$ is estimated as the costs incurred in building the structure (accounting for the geometry of the structure, the materials required, and the cost of labor/machinery to build that structure).

The annual cost of construction C_n is calculated using the following cost comparison equation:

$$C_n = C(m) + \frac{I_0 - C(r)}{n} + \frac{I_0 + C(r)}{2} R_d \quad (2)$$

where $C(m)$ is the maintenance cost, R_d is the discount rate, $C(r)$ is the remaining value of the structure, and n is the service life of a measure. The expression $(I_0 - C(r))/n$ describes imputed depreciation and the expression $R_d(I_0 + C(r))/2$ describes the average imputed interest. For the case study, $C(m)$ is calculated as 5 % of $C(s)$ and 5 % of $C(e)$. These values are taken from personal communications with a consultant in Kathmandu held in November 2019. R_d is assumed to be 12 % based on the upper limit of values used by the World Bank [13] and used in the

Holcombe et al. [19] landslide cost study. The remaining value of the structure $C(r)$ is only applicable to stabilisation measures where the material can be used again post-failure (e.g. masonry walls). In those cases, $C(r)$ is made equal to cost of the material that can be used again (otherwise $C_n = 0$). The service life (time from (re) construction to failure) n is calculated using the method to estimate the frequency of slope failures outlined in Section 2.2.

The overall cost per annum (CE_n) of a stabilisation measure is then calculated as:

$$CE_n = C_n + F_f(I_0 + C(c) + C(d)) \quad (3)$$

where $C(c)$ is the cost of clearing the landslide debris and $C(d)$ is the cost of dismantling the structure. $C(c)$ can be estimated by working out the potential profile failure area of the cut slope (which is assumed to be landslide debris) based on the failure surface determined through a 2-D Limit Equilibrium Method (LEM) stability analysis. The profile-area of the landslide debris is then multiplied by the length of the cut slope (parallel to the road) to determine the landslide debris volume. $C(d)$ accounts for the geometry of the structure and the cost of labor/machinery to dismantle that structure. I_0 is included in this equation as the cost of reimplementing the stabilisation measure after failure. This assumes that the initial cost of construction is the same as the cost of reconstruction after failure, in addition to the cost of clearing the debris after failure and the cost of dismantling the structure. It also assumes that the same stabilisation measure is re-deployed after failure (this assumption is discussed further in Section 2.2). F_f is calculated using the CUTSTAB-P method outlined in Section 2.2.

$C(e)$, $C(s)$, $C(r)$, and $C(d)$ are all specific to the geometry and materials of the slope stabilisation measure implemented and should be based on a region-specific system of rate analysis (see Section 2.3.5 for how this is achieved).

A list of the parameters used in this cost framework is outlined in Table 1. The values given to each of these parameters for the case study is outlined in Table 5.

2.2. CUTSTAB-P method to determine the frequency of slope failure

To determine the annual frequency of slope failure (F_f) we performed the CUTSTAB-P method outlined in Robson et al. [35], which incorporates mechanical Monte Carlo simulation (MCS) probabilistic slope stability analyses coupled with an upslope hillslope-storage Boussinesq (HSB) hydrogeological model. This approach is chosen to enable widespread use of the methodology by practitioners where lack of data often precludes database-focused methods and resource constraints preclude site investigation and monitoring. The overall model accounts for: (1) uncertainty of geotechnical and hydrogeological parameters; (2) rainfall precipitation recorded over a multi-year period of time; and (3) the effect of upslope topography. Morgenstern-Price (M-P) limit

Table 1

The cost-analysis equation parameter descriptions, abbreviations and units. NPR = Nepalese Rupee.

Parameter	Unit	Description
$C(e)$	NPR	Cost of earthworks
$C(s)$	NPR	Cost of structures
$C(m)$	NPR/year	Maintenance costs
$C(r)$	NPR	Remaining value of structure
n	Years	Service life
R_v	%	Value added tax
R_d	%	Discount rate
I_0	NPR	Initial investment
C_n	NPR/year	Annual cost of construction
F_f	#/year	Annual frequency of slope failure
$C(c)$	NPR/year	Cost of clearing the debris
$C(d)$	NPR/year	Cost of dismantling the structure
CE_n	NPR/year	Cost per annum

equilibrium method stability analyses (using Rocscience, Slide2) are performed for the realisations of the geomaterial strength parameters required to calculate the slope probability of failure according to the MCS technique. The MCS is performed to capture variability in slope strength, with a phreatic surface level imposed at a range of heights. These phreatic surfaces are then matched to a phreatic surface time series obtained from the 1D Hillslope-Storage Boussinesq model run for the upslope area to generate Factor of Safety (FoS) time series. From these FoS time series, the annual frequency of slope failure (F_f) is then estimated. The key steps of the CUTSTAB-P method are presented in Fig. 1 and outlined in the following paragraphs in three key stages.

Stage 1 (numerical slope stability analysis and steady-state seepage analysis):

1. Characterise the cut slope according to Generalised Hoek–Brown (G-H-B) failure criterion using field observations and values from literature.
2. Conduct a sensitivity analysis of the parameters to determine which should be varied in a Monte Carlo simulation (MCS).
3. Generate N_r random realisations from the probability distributions of the aleatoric parameters in the MCS, with N_r based on a convergence analysis (Fig. 1a).
4. Define Z, the total head boundary conditions imposed at a range of different heights at the upslope boundary of the cut slope. Conduct Finite Element seepage analyses with Z resulting in N_z phreatic surfaces (Fig. 1b).
5. Conduct N_r deterministic Limit Equilibrium Method (LEM) stability analyses for N_z phreatic surfaces, resulting in $N_z \times N_r$ FoS values. A lookup table can be established with the varied G-H-B parameter set on one axis, and phreatic surface heights on the other, with the values being FoS (Fig. 1c).

Stage 2 (Hillslope-storage Boussinesq, HSB, model):

1. Establish a rainfall time series for the area of interest (Fig. 1e).
2. Determine the HSB slope boundary conditions using a Digital Elevation Model.
3. Generate a lognormal distribution of k based on the potential range of hydraulic conductivities (k) for the geomaterial from published literature (Fig. 1d).
4. Generate N_k realisations of k from the lognormal distribution, with N_k based on a convergence analysis.
5. Solve HSB equation using finite difference method for N_k realisations of k (Fig. 1f), resulting in N_k phreatic surface time series (Fig. 1g).

Stage 3 (combine outputs of stages 1 & 2 to determine a frequency of slope failure):

1. Discretise the phreatic surface time series according to the Z values (Fig. 1h).
2. Express FoS as a discretised function of the phreatic surface for each combination of G-H-B realisation and k realisation (using the FoS lookup table to determine a FoS for each G-H-B parameter set and Z value combination at each phreatic surface timestep) to determine $N_r \times N_k$ FoS time series (Fig. 1i).
3. Convert each FoS time series to a binary ‘failure’ time series with failure being FoS < 1 and stability being FoS > 1.
4. For each FoS time-series, count a landslide when FoS becomes < 1 and then pause counting for a user-defined remediation period, and until the FoS returns to a value 1.
5. Sum the number of landslides across all FoS time series and divide this by the number of FoS time series, $N_r \times N_k$, to estimate the frequency of slope failure over the study period (e.g. 11 years). If this value is normalised by the duration of the study period, the average annual frequency of slope failure (F_f) is obtained.

The CUTSTAB-P methodology is discussed below in more detail.

The cut slope is characterised using the Generalised Hoek–Brown (G-H-B) failure criterion. The material constant (m_i) and unconfined compressive strength (σ_{ci}) account for the strength associated with the rock type. Whilst the Geological Strength Index (GSI) accounts for the strength derived from the structure and surface condition of the rock mass, and the disturbance factor (D) for disturbance of the rock due to excavation (blasting or mechanical). Despite the case study cut slope being excavated by historical blasting, which is likely to have caused some disturbance, D is set to zero to avoid adding further complexity to the example. Note that a key limitation of the G-H-B criterion is its inability to model structurally controlled slope failure since joint-sets are not explicitly accounted for. However, the methodology here presented can be applied to structurally controlled slope failures without any loss of generality. To do so, would require inclusion of the relevant geological structures controlling failure (e.g. faults and joint-sets) within the slope stability analysis. This is feasible in computational terms within Rocscience, Slide2 and many other stability programmes, but is challenging in terms of acquiring the field data to parameterise the models.

A sensitivity analysis was conducted on the G-H-B criterion to determine which parameters the model was most sensitive to and, therefore, which should be varied as part of the MCS. To do so, literature-based estimates for the upper, lower limit, and midpoint of each parameter were input into the model (tested one at a time), and a standard deviation (STDEV) calculated using the output FoS (for the upper, lower limit, and midpoint values) was computed for each parameter. In our case, we found that the model is most sensitive to the Geological Strength Index (GSI) [9,24].

A lognormal distribution of GSI is characterised according to the 1st and 99th percentiles being the lower and upper limits established for GSI (based on field observation and literature values), respectively. A lognormal distribution is chosen to avoid negative values. Characterising the distribution according to 1st and 99th percentiles allows for occasional occurrence of values outside the typical range. 1000 realisations (i.e. $N_r = 1000$, determined through a convergence analysis) of GSI are derived from its probability distribution to use in the probabilistic stability analyses. Note that in cases where more than one geotechnical parameter is stochastic, a methodology for parsimonious sampling in the space of the stochastic geotechnical parameters would be required (e.g. latin hypercube sampling).

For each stabilisation measure tested, a separate set of slope stability analyses (using the same stochastic parameter sets) is performed for a number of phreatic surface levels to capture potential variability in the height of the phreatic surface. The phreatic surface is generated using Finite Element (FE) steady state seepage analysis in Slide2 with a total head boundary condition of Z on the upslope boundary, carried out prior to the deterministic stability analyses. The external boundaries and mesh used in the model are determined by convergence analyses. The range of Z values included are from a minimum where the phreatic surface no longer influences the cut slope’s stability (i.e. FoS) to a maximum where the phreatic surface is at the ground surface. The spacing between Z values is set by the mesh element size since the phreatic surface is insensitive to spacing more granular than this.

The next step is to determine the frequency with which the cut slope experiences the different phreatic surfaces over time. To do so, a phreatic surface time series is derived at the location of upslope boundary of the stability model. This is achieved using 11 years of daily rainfall data and the HSB model, a reformulation of the Boussinesq equation (the continuity and Darcy equations) in terms of water storage [41]. In this form, the 3-D flow problem can be reduced to a 1-D problem so that the runtime of the numerical solution is affordable. The equations are written in terms of a variable width function along the x-axis ($w(x)$) which is given by the expression $w(x) = w_0 \exp[\beta x]$ (Troch et al. [41] p. 7) where w_0 is the width at $x = 0$ and β is a shape factor controlling the variation of the width along the x-axis.

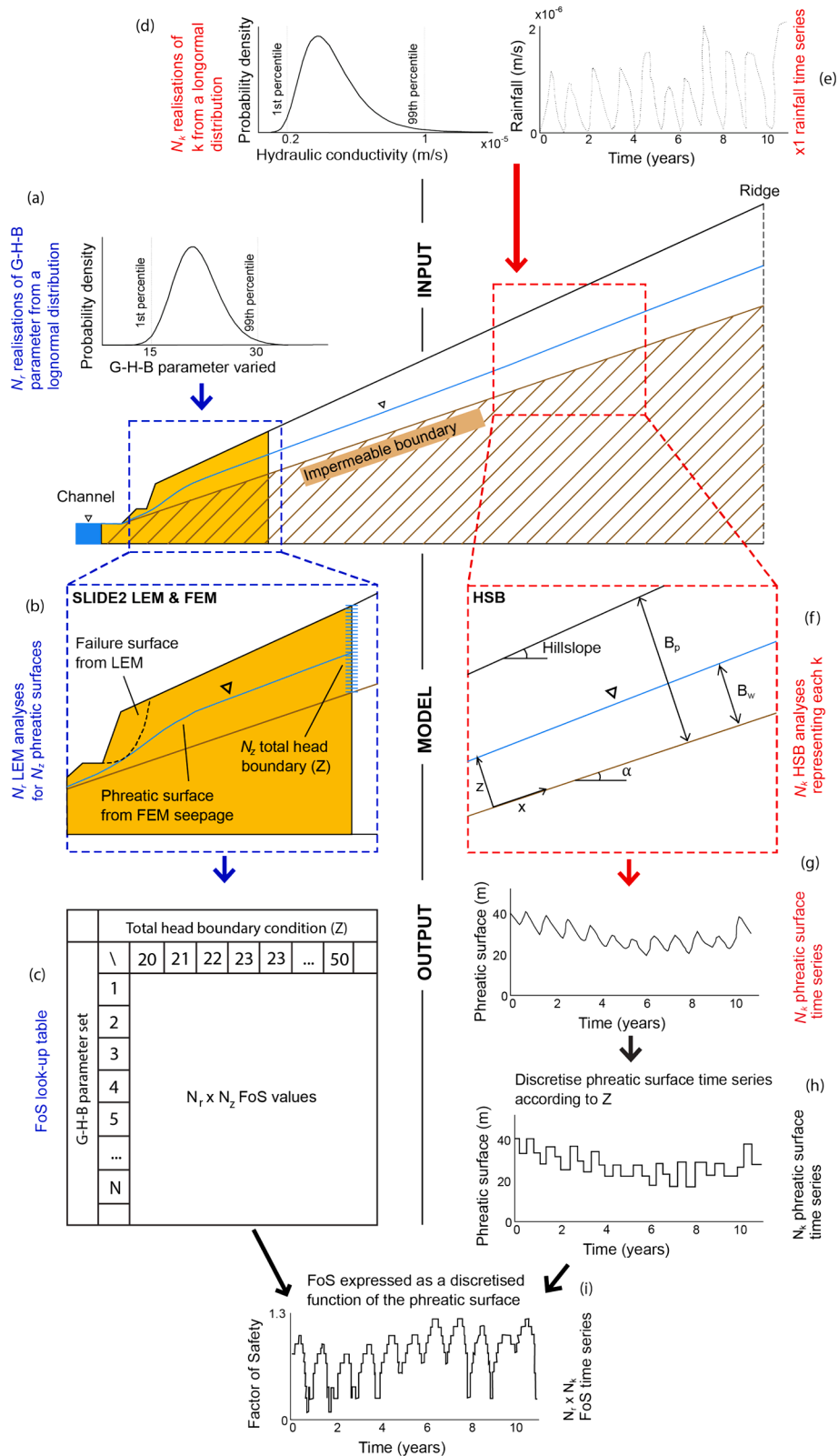


Fig. 1. A schematic diagram adapted from Robson et al. [35] highlighting the key elements of the CUTSTAB-P method to determine the frequency of slope failure. The probabilistic model is the system highlighted in blue and the hillslope-storage Boussinesq (HSB) model is the system highlighted in red. The yellow area of the slope shows the stability model domain. The outputs of the two models are coupled to express FoS as a discrete function of the phreatic surfaces. (For interpretation of the references to colour in this figure legend, the reader is referred to the web version of this article.)

The HSB model assumes uniform hydraulic conductivity over an impermeable geomaterial with the boundary between the two layers being a constant inclination (α). The thickness of the permeable layer at the upslope boundary of the `Slide2` model is described by (B_p), so that the impermeable boundary is at the level of the river channel at the river channel. The HSB equation of Troch et al. [41] (outlined in Robson et al. [35]) is solved numerically in a finite difference scheme to generate a phreatic surface time series from the rainfall time series. Initial phreatic surface height is assumed to be at the impermeable boundary, in the absence of other information; storage at the outlet is fixed at zero and there is a no-flow boundary at the ridge. The 11-year rainfall record is duplicated resulting in a 22-year time series to remove any sensitivity to the initial conditions on the subsurface flux. In our model, the rainfall is regarded as recharge to the groundwater table and does not consider infiltration processes and their effect on matric suction. This is appropriate for assessing rock cut slope stability where matric suction would constitute only a small part of the material strength. This method would need further work to be adapted to slopes where matric suction-derived strength dominates.

Hydraulic conductivity (k), a key parameter within the HSB model, is highly variable. Therefore, the equation is solved using 2000 k realisations (i.e. $N_k = 2000$, which is the minimum number of k values required to have $\leq 1\%$ difference in the output) taken from a lognormal distribution of k . A lognormal distribution was chosen to avoid physically impossible negative k values. The lognormal distribution for k is parameterised so that its 1st and 99th percentiles are at the lower end and upper end of potential k values for the geomaterial (see Section 2.3.4 for case study values). The material porosity (n_f) is taken as an average of literature values for the geomaterial type. The shape factor (β) and length of the hillslope (L) are determined by examining a Digital Elevation Model (DEM) of the hillslope in ArcGIS.

The output of this HSB model set up is 2000 phreatic surface time series, of the same duration as the input rainfall time series. While the HSB model is dynamic in the sense that it has time-varying rainfall input, the timestep is daily in our application. The slowly varying phreatic surface predictions from the HSB model can be considered a set of sequential steady states. The same set of phreatic surface time series can be used for all the stabilisation measures.

The final step is to combine the outputs of the probabilistic and HSB models. To do so, the phreatic surface time series are discretised according to the Z values that were used to generate the phreatic surfaces for the MCS. The indices determined for discretisation of the phreatic surface time series are used to express the FoS output from the probabilistic analyses as a function of phreatic surface (using the FoS lookup table to determine a FoS for each G-H-B parameter set and Z value combination at each phreatic surface timestep) that can then be used to generate a unique FoS time series for each realisation of the geotechnical parameters (GSI) and each realisation of k . Each FoS time series is converted to a binary ‘failure’ time series with failure for $\text{FoS} < 1$ and stability for $\text{FoS} > 1$. Each ‘failure’ time series is worked through chronologically so that when the FoS values drops below 1, we count this as a failure for that time series. Then after a number of remediation days (preventing further failures from being counted) to allow time for cut slope to be reinstated in its previous geometry, we resume the working with any successive failure counted again. We include a clause in the code that says if the remediation period finishes when the slope $\text{FoS} < 1$, counting does not resume until the FoS recovers to 1. This method assumes that the slope is restored to its previous geometry. This is unlikely to be the case, however, the geometry after failure is unknown without further analyses which would also be highly uncertain. Given this uncertainty, we define failure events in terms of their impact on the road thus we say that new failures are those that occur after sufficient time for remediation to have taken place on the slope. Our method also assumes that the previous stabilisation measure is implemented again after failure. Re-implementing the same stabilisation

measure after failure is a common occurrence in Nepal, particularly for retaining walls [33]. However, this assumption is less true in the context of a higher-income country.

The total number of landslides is then summed across all ‘failure’ time series and divided by the number of slope geotechnical parameter realisations and the number of k realisations (i.e. total number of landslides/ (1000 \times 2000)) to determine the frequency of failures. This value can be further divided by the number of years to give the annual frequency of failures (F_f). The resulting F_f for each stabilisation measure can be used to determine the cost of the undesired consequences. The service life (n) can be calculated as the total time of the study (total rainfall time series) divided by the frequency of failure for the study period.

2.3. Case study

2.3.1. Background to cut slopes in Nepal

Nepal is situated within the central part of the Himalayan arc, a hotspot for fatal landslides that are associated with active tectonics and periods of heavy rainfall. Landslides in Nepal are predominantly triggered either by earthquakes, which are rare but can trigger hundreds to thousands of landslides, or by rainfall, which triggers many landslides in Nepal every year with 93 % of landslides in Nepal occurring during the four-month monsoon season [10]. However, the susceptibility of slope failures in Nepal is exacerbated by poorly planned road alignments, haphazard construction of roads, and a lack of slope stabilisation measures [22,10,34]. This can be observed within the strategic and local road networks of Nepal [38,31,18]. McAdoo et al. [26] found that rainfall-triggered landslides are up to two times more common along poorly constructed roads as compared to areas without such roads.

There has been a global push to expand infrastructure networks for example through the Sustainable Development Goals where “the proportion of the rural population who live within 2 km of an all-season road” is explicitly defined as an indicator (SDG Indicator 9.1.1.) [42]. This is reflected in Nepal with sustained and ongoing national-scale investment into growing the road network with government plans to expand the road network by c. 140 % from 2015 to 2030 [27]. But interviews and surveys with stakeholders in Nepal including consultants, contractors, governing officials, donor agencies, and construction workers suggest that: (1) road slope stabilisation is not a priority in road projects; (2) there is poor communication between stakeholders; and (3) there is no means to justify resources towards slope stabilisation [33]. Therefore, a substantial amount of this investment is lost when the roads are not built adequately or without taking slope stability into account. Rural Access Programme (RAP) Phase 3 suggest that by 2011 55 % of the Lower Road Network in Nepal that had been constructed since 2000 was unusable due to a lack of maintenance (including slope stabilisation) resulting in estimated investment losses equivalent to USD 1 billion (US Dollar) [31].

2.3.2. Case study site description

We demonstrate the methodology presented in this paper on a cut slope situated along the Narayanghat-Mugling road in Chitawan, Nepal (Fig. 2). A field assessment (including geotechnical, geological and geomorphological observations) was conducted at the site in November 2019. At this site, there is an above-road full-cut slope (i.e. no fill) of around 25 m in height and 70° inclination made up of weathered phyllite (identified based on geological observation). The cut slope is located 15 m upslope from the river Trishuli. The hillslope is inclined at c. 25° above the cut slope, is slightly convex in profile and convex in plan. This road was originally excavated by blasting around 40 years ago (personal communications with consultants working on the road in November 2019). A 2 m tall gabion wall constructed along the base of this cut-slope collapsed due to a minor landslide during the 2019 monsoon season.

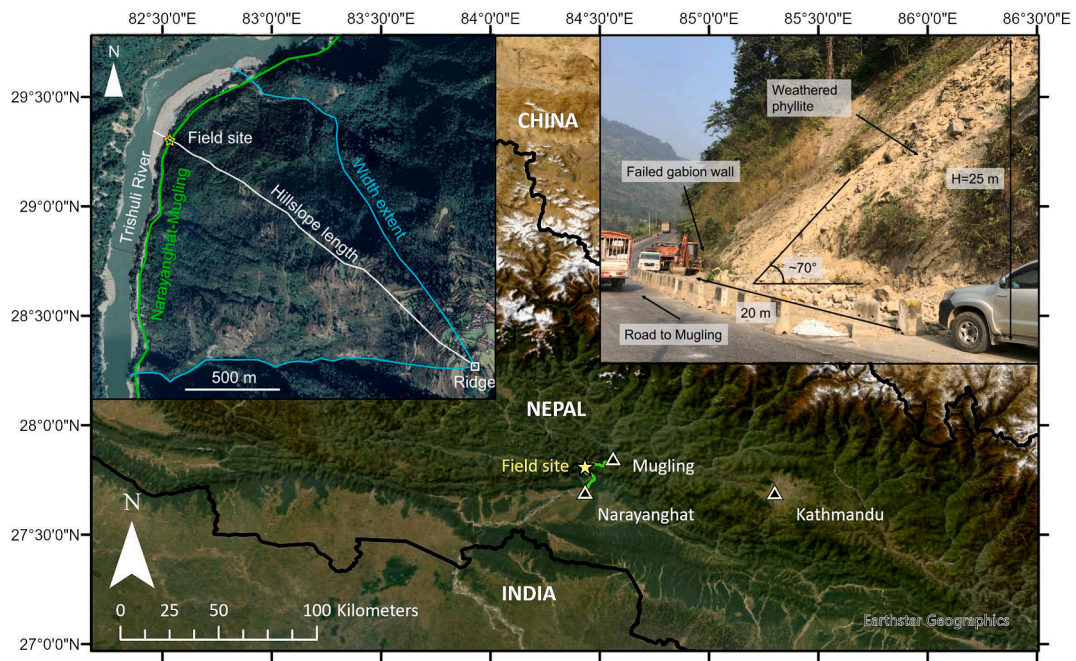


Fig. 2. Map of Nepal with field site highlighted along the Narayanghat-Mugling road, including an inset map of the field site catchment and an image of the field site (image taken in November 2019).

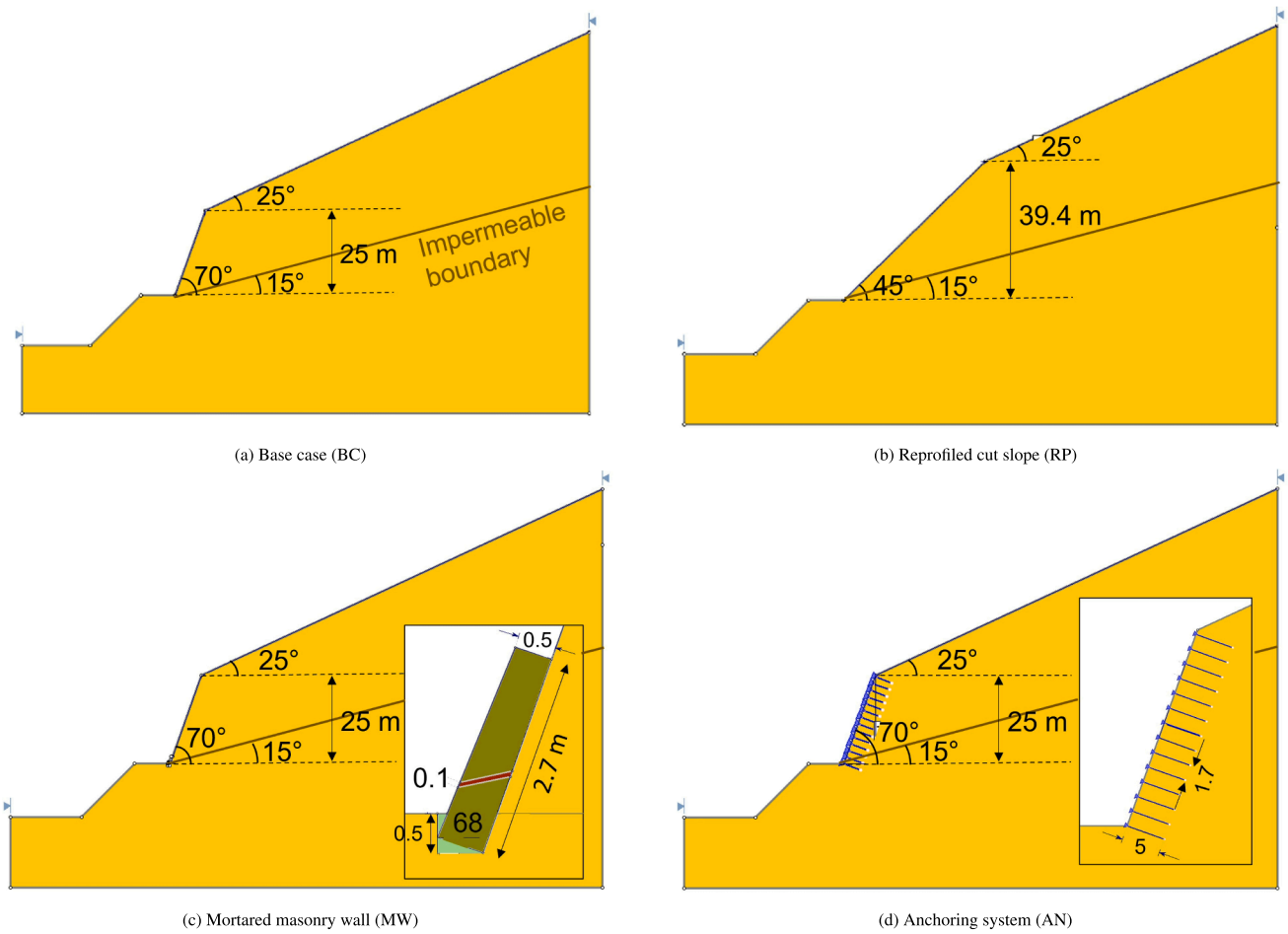


Fig. 3. Rocscience, Slide2 LEM model set up for each case: (a) the base case (BC) with a cut slope of 70° inclination and 25 m in height, whilst hillslope is 25°; (b) the reprofiled cut slope (RP) to 45° based on Nepali guidelines [4] (hillslope remains at 25°); (c) mortared masonry wall (MW) designed according to common geometry observed in Nepal (maintains 70° cut slope inclination); and (d) the anchoring system (AN) with 14 5 m anchors spaced 1.7 m.

2.3.3. Stabilisation measures

Our cost analysis methodology is used to assess the cost efficiency of four slope stabilisation measure scenarios that can be found in Nepal for our case study site. Each stabilisation measure has the following design details (the LEM slope model in Slide2 for each stabilisation measure is presented in Fig. 3):

- 1. Base case (BC):** the cut slope with no measures is 25 m in height inclined at 70° with a hillslope inclination of 25°.
- 2. Reprofiled (RP):** the cut slope is reprofiled to an angle of 45°, recommended in a Nepali Government manual [4]. Table C3.6 of the manual provided by Department of Roads [4] (Annex C, p. 12) outlines cut slope angle guidelines for cut slopes that have a rock mass with no structural control. Given that the cut slope in the case study exhibits a blocky mass with highly weathered rock, Table C3.6 advises an inclination of 45°. The cut slope height is 39.4 m and the hillslope inclination of 25° maintained.
- 3. Mortared masonry wall (MW):** a mortared masonry wall is implemented at the toe of the cut slope with the geometry commonly observed along roads visited in Nepal (i.e. not designed based on the slope conditions): around 2.5 m in height and a top width of 0.5 m. During multiple field visits, it was observed that masonry walls were often inclined resting on the slope face with no backfill between wall and slope, and were constructed to a depth of 0.5 m below the road surface. The cross-sectional area of the wall is 1.5 m² and the length of the wall parallel to the road is 20 m. The area surrounding the base of the wall is infilled with backfill with geotechnical parameters inferred from bidding documents for works on the Narayanghat-Mugling road ($c = 0$ kPa, $\phi = 34$ and $\gamma = 17.5$ kN/m³). The volume of backfill required is 2.44 m³. The wall itself is designed to strength specifications for a mortared masonry wall outlined in Department of Roads [4] ($c = 65$ kPa, $\phi = 30$ and $\gamma = 24.4$ kN/m³). A weep hole is implemented with a width of 0.1 m around 0.5 m above ground as per observations and designed with the same geotechnical parameters as the wall, but with $k = 1 \times 10^{-4}$ m/s. The geometry of the cut slope and slope remains consistent with the base case.
- 4. Anchors (AN):** An anchoring system is designed based on a rate analysis document for the Narayanghat-Mugling road (Department of Roads, Narayanghat-Mugling Road Project, Chitwan, Rate Analysis, Fiscal Year 2017/18): end-anchored bars 5 m in length, with spacing at 1.5–2 m intervals (1.7 m) up the cut slope, 2 m out-of-plane spacing and inclined normal to the slope surface. This report points to the use of tendons supplied by DYWIDAG Systems International that have a capacity of 270 kN. If the cut slope had an obvious foliation geometry, the orientation of anchors would need to be designed to account for this. In this case, there was no obvious foliation geometry so they were installed orthogonal to the cut slope. The geometry of the cut slope and slope remains consistent with the base case.

2.3.4. Frequency of failure of the case study stabilisation measures

We followed the CUTSTAB-P methodology outlined in Section 2.2 to determine a F_f for every stabilisation measure. We evaluated the range of GSI and σ_{ci} values for the cut slope in the field using the guidelines of Marinos & Hoek [24]. We then determined typical ranges of values for weathered phyllite from literature: unit weight, γ , from Fine [9] and m_i from Marinos & Hoek [24]. Estimates of reasonable upper and lower limits of each parameter are outlined in Table 2.

GSI is varied as part of the MCS based on the results of a sensitivity analysis (carried out using the base case, BC). The GSI for this slope is relatively low (15–30) as the rock mass was heavily fractured due to weathering. As a result, the rock mass towards the surface does not manifest any dominant structural orientation controlling failure. 1000 stability analysis realisations are performed using GSI values (i.e. $N_r =$

Table 2

Reasonable estimates for the upper and lower limits of unit weight (γ) and the Generalised Hoek–Brown (G-H-B) parameters for a cut slope made up of phyllite on the Narayanghat-Mugling road based on field observations and values from literature. The G-H-B failure criterion include: Geological Strength Index (GSI), material constant (m_i), and unconfined compressive strength (σ_{ci}). Values used in the MCS are also shown. GSI is varied as part of the MCS, while the values of γ , m_i and σ_{ci} are held constant.

		Lower limit	Upper limit	Reference	Values used
γ	[kN/m ³]	23	25	Fine [9]	24 (constant)
GSI	[-]	15	30	Marinos & Hoek [24]	15→30 (varied)
m_i	[-]	4	10	Marinos & Hoek [24]	7 (constant)
σ_{ci}	[MPa]	15	35	Marinos & Hoek [24]	25 (constant)

1000) sampled from a lognormal distribution with its 1st and 99th percentiles being the lower and upper limits established for GSI, respectively. The same set of 1000 GSI values are used for all the stabilisation measures analysed. The other G-H-B parameters (excluding GSI) are held constant for each stability analysis (see Table 2 for values).

For each stabilisation measure, a FE steady seepage analysis model is set up in Slide2. Based on the mesh size (determined by convergence analyses), 25 Z values (i.e. $N_z = 25$) can be implemented as upslope phreatic surface boundary conditions between a minimum phreatic surface that no longer influences the cut slope's stability (47.5 m below the ground surface) and a maximum where the phreatic surface is at the ground surface itself. A separate set of MCS runs (using the same stochastic parameter sets) is performed for each of the 25 seepage scenarios. Thus for each stabilisation measure and phreatic surface scenario an MCS of 1000 deterministic stability analyses are conducted using the same set of 1000 GSI values sampled from a lognormal distribution.

The frequency with which the cut slope experiences each of the 25 different phreatic surfaces over time is estimated using the HSB model driven by: a rainfall time series, estimates of k and n_f , and an estimate of the shape of the hillslope. Daily rainfall data spanning an 11-year period from 2010 to 2020 (but missing data for 2013) was purchased from the Government of Nepal Department of Hydrology and Meteorology (www.dhm.gov.np) for Sakhar meteorological station in the district of Tanahun c. 13 km from the cut slope at an elevation c. 60 m higher than the road at the cut slope. Singhal & Gupta [39] suggest that variability in k is likely positively skewed with k values in the range 10^{-9} to 10^{-5} m/s for crystalline, low-grade metamorphic rock (i.e. phyllite). Thus, given uncertainty in k and lack of measurements at this site (as is typical for road cut slopes in Nepal and LMICs in general), these values were used as the initial 1st and 99th percentiles for a lognormal k distribution. However, this lower limit was found to produce excessive extent and frequency of surface saturation inconsistent with field observations at the site, which suggest overland flow rarely or never occurs on the cut slope. Thus the 1st percentile was increased to a value where the cut slope would not experience sustained periods of surface saturation (i.e. phreatic surface at the ground surface). The final 1st percentile of k was 1.7×10^{-6} m/s. 2000 realisations of k were established from this lognormal distribution (i.e. $N_k = 2000$).

The material porosity (n_f) is taken as an average of literature values for phyllite as it is less variable than k [39]. A Shuttle Radar Topography Mission (SRTM) DEM of 1-arc second resolution of the hillslope in ArcGIS is used to determine L (the length of the catchment area) and β (best fitting exponential for observations of the hillslope width at three points upslope of the cut slope), which are measured by hand. We assume that the weathered bedrock is underlain by unweathered rock of such low permeability as to be functionally impermeable and that the permeable weathered bedrock thickness tapers downslope so that it is thickest at the ridge [40]. Therefore, it is assumed that the impermeable

boundary intersects the ground surface at the river channel below the cut slope (the downslope boundary of the hillslope) and is inclined at 15° , 10° lower than the ground surface, resulting in a permeable layer thickness of c. 51 m at the upslope boundary of the Slide2 model.

The key input parameters for the HSB model for this case study are outlined in Table 3.

The output of this HSB model setup is 2000 phreatic surface time series each of 11-year duration and daily resolution. The output of the probabilistic stability analysis and the HSB model are combined to determine a F_f for each stabilisation measure (using the methodology outlined in Section 2.2) and presented in Section 3. A 90-day period is implemented as the remediation time, the period after a landslide has occurred during which the cut slope is being or is yet to be remediated. This is an assumption based on the monsoon season lasting between three and four months in Nepal, during this time work cannot be carried out.

2.3.5. Case study costings

The costs for each stabilisation measure are estimated using the system of rate analysis from Nepal to give standardised contract costing estimates for budgeting and tendering purposes. The rates vary from region to region across Nepal. Table 4 outlines the key rates used for the cost calculations taken from a rate analysis document for the Narayanghat-Mugling road (Department of Roads, Narayanghat-Mugling Road Project, Chitwan, Rate Analysis, Fiscal Year 2017/18) collected from the Department of Roads project manager working along the Narayanghat-Mugling road during fieldwork in November 2019. These costs incorporate those for labour, material, and equipment.

The cost of the structure ($C(s)$) for the wall is calculated by determining the volume of the wall at the site and multiplying by the unit cost of the construction of a stone masonry wall (unit cost from the Department of Roads, Narayanghat-Mugling Road Project, Chitwan, Rate Analysis, Fiscal Year 2017/18). This is added to the volume of the backfill multiplied by the unit cost for backfill for a stone masonry wall and the geometry of foundations multiplied by the foundations excavation for SM wall. $C(s)$ for the anchoring system was calculated by multiplying the size of the slope covered by anchors (26.55 m) by their length (5 m) by the unit cost for the installation of anchors (the unit cost for the installation of anchors asks for this method in the rate analysis documents). The cost of dismantling the wall ($C(d)$) was calculated by multiplying the volume of the wall by the unit cost for dismantling stone masonry in cement mortar (unit cost from the Department of Roads, Narayanghat-Mugling Road Project, Chitwan, Rate Analysis, Fiscal Year 2017/18). The cost of earthworks ($C(e)$) for the reprofiled case was determined by calculating the volume of material to be excavated to achieve the lower inclination from the BC and multiplying this by the unit cost for excavation and disposal of earthworks (unit cost from the Department of Roads, Narayanghat-Mugling Road Project, Chitwan, Rate Analysis, Fiscal Year 2017/18). The cost of clearing landslide debris ($C(c)$) was calculated as the volume of failed material (failure area for the most critical failure from Slide2 multiplied by the length of the cut slope) for each stabilisation measure multiplied by the unit cost for landslide clearance and material haulage, in addition to the trimming of unstable material (unit cost from the Department of Roads,

Table 3

Case study input parameters for the HSB model. The inclination of impermeable boundary (α) is assumed to be less than the inclination of the hillslope, and the thickness of the permeable boundary (B_p) is worked out based on α . The shape factor (β), initial width (w_0) and length of slope (L) are estimated from a DEM in ArcGIS. Porosity (n_f) is taken as an average of crystalline metamorphic rock from literature.

B_p [m]	α [°]	β –	w_0 [m]	L [m]	n_f [%]
51.28	15	–0.0008	1619.9	1457.0	7.5

Table 4

Table of key unit costs for slope stabilisation, relevant to this analysis, taken from a rate analysis document for the Narayanghat-Mugling road (Department of Roads, Narayanghat-Mugling Road Project, Chitwan, Rate Analysis, Fiscal Year 2017/18). Abbreviations: SM = Stone Masonry, dia. = diameter, and NPR = Nepalese Rupee.

Description of works	NPR/unit
Excavation including disposal with excavator (m ³)	252.00
Rubble SM of hard stone in 1:4 cement sand mortar (m ³)	8041.00
Foundations excavation for SM wall (m ³)	252.00
Backfill for SM wall (m ³)	411.00
Installation of anchors (Fe 500D dia. 25 mm) (m)	5029.93
Landslide clearance and material haulage (m ³)	191.00
Trimming unstable material (m ³)	154.45
Dismantling SM in cement mortar (m ³)	902.17

Narayanghat-Mugling Road Project, Chitwan, Rate Analysis, Fiscal Year 2017/18). All the geometries used in the costings for each stabilisation measure are outlined in Table 5.

3. Results

By conducting the CUTSTAB-P method outlined in Section 2.2, F_f for each stabilisation measure is estimated and outlined in Table 5. An estimation for the service life (n) of each stabilisation measure is calculated as the total time of the study (11 years) divided by the frequency of failure for the study period (outlined in Table 5).

These F_f are used to calculate the cost per annum (CE_n) for each stabilisation measure using the equations outlined in Section 2.1 with the unit costs from the rate analysis for the region (outlined in Table 4) and the specific geometries for each of the stabilisation measures (outlined in Table 5). The results are outlined in Table 5.

Based on the best estimate for the model parameters, it is found that the stabilisation measure with the lowest cost per annum (i.e. most cost-efficient) is the anchoring system (AN). The next most cost-efficient stabilisation measure is the base case (BC) closely followed by the reprofiled cut slope (RP). The least cost-efficient measure (i.e. highest cost per annum) is the mortared masonry wall (MW). By implementing the AN for this cut slope rather than MW, it is estimated that NPR 221,767 (Nepalese Rupee), equivalent to USD 1,665 (US Dollars), would be saved annually on direct costs (a saving of 72 % relative to total annual costs for MW). If this cost optimisation is carried out for cut slopes across Nepal, total savings could be substantial. These outcomes are further discussed in Section 3.1. The sensitivity of these results to the model input parameters that are based on assumptions (99th percentile value for k , the porosity, the inclination of the impermeable boundary and the 90-day remediation period) is discussed in Section 3.2.

3.1. Outcomes

By following the methodology presented in this paper, the most cost-efficient stabilisation measure for the cut slope based on the chosen input parameters is AN. The next most cost-efficient scenario is BC. Despite BC being cost-efficient in terms of direct costs, this scenario could have high indirect costs as it results in the highest F_f . How the inclusion of indirect costs might change the results is explored in Section 4.2. RP is the third most cost-efficient of the four stabilisation measures. However, it is not clear whether there would be room upslope of the cut slope to excavate it to the inclination required. MW is the least cost-efficient stabilisation measure tested, despite having lower initial investment costs than RP and AN, due to its high F_f .

3.2. Sensitivity to input parameters

In this paper, the key assumptions that we made in preparing the

Table 5

This table includes: (1) geometries for each stabilisation measure used to calculate cost; (2) annual frequency of failure (F_f) and service life (n) for each stabilisation measure estimated using the method outlined in Section 2.2; (3) parameter values used to determine the cost per annum (CE_n) for each stabilisation measure scenario; and (3) CE_n calculated using the equations outlined in Section 2.2. The cell colour scale is from dark green to yellow, where dark green is the most cost-efficient stabilisation measure (lowest CE_n) and yellow indicates the least cost-efficient stabilisation measure (highest CE_n). NPR = Nepalese Rupee and USD = US Dollar. Exchange rate 1 NPR = 0.0075 USD.

Parameter	Symbol	Unit	BC	RP	MW	AN
			Base case	Reprofiled	Masonry wall	Anchors
Volume of excavated material		m ³	-	6436.90	-	-
Volume of structure		m ³	-	-	30.00	-
Volume of backfill		m ³	-	-	2.44	-
Volume of foundations		m ³	-	-	10.00	-
Anchors		m	-	-	-	132.74
Volume of potential failure material		m ³	1143.46	6088.22	1254.80	6726.46
Annual failure frequency	F_f	Failures/year	0.46	0.00055	0.39	0.0023
Service life	n	Years	2.16	1803.28	3.48	438.25
Cost of earthworks	$C(e)$	NPR	0	1,622,099.00	0	0
Cost of structures	$C(s)$	NPR	0	0	244,752.80	667,606.54
Maintenance costs	$C(m)$	NPR/year	0	81,104.94	12,237.64	33,380.33
Remaining value of structure	$C(r)$	NPR	0	0	48,780.00	0
Service life	n	Years	2.16	1803.28	3.48	438.25
Value added tax	R_v	%	13	13	13	13
Discount rate	R_d	%	12	12	12	12
Initial investment	I_0	NPR	0	1,832,972.00	276,570.70	754,395.40
Annual cost of construction	C_n	NPR/year	0	192,099.70	97,246.44	80,365.44
Cost of clearing the debris	$C(c)$	NPR/year	183,147.37	1,166.31	124,618.87	5,304.52
Cost of dismantling the structure	$C(d)$	NPR/year	0	0	7780.97	0
Cost per annum	CE_n	NPR/year	183,147	194,282	309,158	87,391
Cost per annum	CE_n	USD/year	1,375	1,459	2,322	656

inputs for the HSB model are: (1) that the 99th percentile value for k is one of the highest values in the range for fractured crystalline metamorphic rock outlined in Singhal & Gupta [39]; (2) that the porosity was the average of the range of values stated by Singhal & Gupta [39]; (3) that the impermeable boundary is inclined at a particular angle; and (4) that remediation of the slope takes 90 days. The sensitivity of the CBA model to each of these assumptions is tested by carrying out one-at-a-time sensitivity analyses.

The lognormal distribution of k (from which values of k are taken for the HSB model) is defined according to 1st and 99th percentiles. The value for the 1st percentile was then set based on the observational constraint that the cut slope had no evidence of overflow. For the case of the 99th percentile, there is no observational constraint and, therefore, it is assumed that this value is at the higher end of values found in literature ($k = 1 \times 10^{-5}$ m/s from Singhal & Gupta [39]). The sensitivity of the model to this value is tested (results displayed in Table 6). It is found that either BC or AN are always the most cost-efficient, and RP or MW

are always the least cost-efficient. In the cases of BC and MW the lower the value of the 99th percentile of k , the higher the CE_n . However, this trend is not observed in the cases of RP and AN as there is very little difference in the F_f between each value of k and, therefore, very little difference in the CE_n . The maximum sensitivity, expressed as the maximum percentage difference in CE_n from k values tested compared to the original value (i.e. $k = 1 \times 10^{-5}$ m/s) is 2 % for BC, 8 % for AN, 52 % for BC and 46 % for MW. From 6.0×10^{-6} to 1.8×10^{-5} m/s, AN is the most cost-efficient stabilisation measure. For 2.2×10^{-5} m/s, BC is most cost-efficient and is 7 % more efficient than AN. From 6.0×10^{-6} to 1.4×10^{-5} m/s, MW is least cost-efficient; but from 1.8×10^{-6} to 2.2×10^{-5} m/s, RP is least cost-efficient.

The sensitivity of CE_n to the value of porosity used in the HSB model is also tested. Porosity was assumed to be 7.5 % based on the average for values of crystalline metamorphic rock in literature (ranging from 5 to 10 % according to Singhal & Gupta [39]). Table 7 outlines the results of

Table 6

Sensitivity analysis of the cost per annum (CE_n) of the 99th percentile defining the lognormal distribution of hydraulic conductivity (k). The cell colour scale is from dark green to yellow, where dark green is the most cost-efficient stabilisation measure (lowest CE_n) and yellow indicates the least cost-efficient stabilisation measure (highest CE_n). NPR = Nepalese Rupee.

k m/s	BC	RP	MW	AN
	Base case NPR/year	Reprofiled NPR/year	Masonry wall NPR/year	Anchors NPR/year
6.0×10^{-6}	244,772	194,440	410,998	87,984
1.0×10^{-5}	183,147	194,282	309,158	87,391
1.4×10^{-5}	117,242	194,859	203,028	88,576
1.8×10^{-5}	93,358	193,181	167,809	84,394
2.2×10^{-5}	88,090	197,272	166,739	94,780

Table 7

Sensitivity analysis of the cost per annum (CE_n) to the porosity of the cut slope. The cell colour scale is from dark green to yellow, where dark green is the most cost-efficient stabilisation measure (lowest CE_n) and yellow indicates the least cost-efficient stabilisation measure (highest CE_n). NPR = Nepalese Rupee.

Porosity %	BC	RP	MW	AN
	Base case NPR/year	Reprofiled NPR/year	Masonry wall NPR/year	Anchors NPR/year
5	182,551	200,261	331,772	102,203
7.5	183,147	194,282	309,158	87,391
10	161,781	192,657	265,194	83,140

a sensitivity analysis on how the porosity affects CE_n for each stabilisation measure. This analysis shows that across the reasonable range of porosity values the most cost-efficient measure is always AN, and the least cost-efficient measure is always MW.

As mentioned in Section 2.3.4, the inclination of the impermeable boundary is assumed to be 15° so that the permeable layer thickens towards the ridge of the slope. The sensitivity of CE_n to the inclination of the impermeable boundary is outlined in Table 8. In each case, B_p is changed with the inclination to ensure that the impermeable boundary intersects the ground surface at the river channel. The analysis shows that the greater the inclination, the greater the F_f and the greater the CE_n . An increased inclination of the impermeable boundary results in a higher phreatic surface (because the permeable layer is thinner in the vicinity of the cut slope), therefore, resulting in greater numbers of failures in the stability model. For inclinations of 15° and 20° , AN is the most cost-efficient; for 25° RP is most cost-efficient (the F_f is significantly lower in RP than the rest of the stabilisation measures). In all cases, MW is the least cost-efficient measure.

The sensitivity of the CE_n to the number of remediation days is also tested. In the methodology, 90 remediation days are assumed based on the duration of the monsoon season in Nepal. Table 9 shows the results of a sensitivity analysis on the number of remediation days. AN is the most cost-efficient of the stabilisation measures from 7 to 270 days, but BC is the most cost-efficient for the case of 365 days. MW is the least cost-efficient from 7 to 180 days, then RP from 270 to 365 days. This analysis shows that, for all stabilisation measures, F_f and CE_n decreases with increasing remediation time. AN is most cost-efficient until the F_f is low, and then BC is most cost-efficient.

In assessing all of the outcomes of the one-at-a-time sensitivity analyses, AN is the most cost-efficient scenario in 84 % of cases, BC in 11 % and RP in 5 %. Indirect costs could play a much larger role in the cost efficiency for BC, as the frequency of failures is high, and therefore, the cost from road closure will be high (discussed in Section 4.2). MW is the least cost-efficient scenario in 79 % of cases, and RP in 21 %. The case of 7 remediation days (F_f highest) results in the greatest difference in CE_n between scenarios: implementing MW would cost NPR 3,275,831 per year compared to 145,172 for AN.

Table 8

Sensitivity analysis of the cost per annum (CE_n) to the inclination of the impermeable boundary. The cell colour scale is from dark green to yellow, where dark green is the most cost-efficient stabilisation measure (lowest CE_n) and yellow indicates the least cost-efficient stabilisation measure (highest CE_n). NPR = Nepalese Rupee.

Inclin- -ation °	BC	RP	MW	AN
	Base case NPR/year	Reprofiled NPR/year	Masonry wall NPR/year	Anchors NPR/year
15	183,147	194,282	309,158	87,391
20	490,449	204,037.53	896,438	113,947
25	1,269,129.21	380,362.78	2,797,900	581,039

4. Discussion

4.1. Choices

This CBA finds that the mortared masonry wall (MW) designed to a standard geometry, is the least cost-efficient stabilisation measure for this cut slope. However, through multiple field trips in Nepal, it was found that this measure is extremely common, especially on the local road network. This may be due to the relatively low initial investment for constructing a mortared masonry wall compared with an anchoring system or reprofiling a cut slope. In addition, materials for such a wall can be sourced locally and the construction requires relatively low-skilled labour. The reprofiled cut slope was found to be the third most cost-efficient, with a CE_n very close to the base case. However, only one inclination for this reprofiled cut slope was tested, and it has been found through multiple field trips that cut slopes are often steeper than recommended in the Nepali guidelines [4]. It may be that a steeper inclination, that requires less excavation but remains stable may be more cost-efficient. Anchoring systems for cut slope stabilisation can only be found on major highways on the strategic road network of Nepal (e.g. the Narayanghat-Mugling road). This CBA finds that AN is the most cost-efficient measure based on direct costs, despite having the second-highest investment costs. It is important to note that anchoring systems are not necessarily the best possible measure for the study cut slope, they are just better than the others tested in this analysis (the base case, reprofiling, and a mortared masonry wall of standard geometry). There are many other alternative stabilisation measures (or even combinations of measures) that could be tested and these might be better still e.g. reprofiling to a different geometry (a different angle or benched profile), bioengineering, gabion or concrete walls, or different drainage solutions.

The sensitivity analysis highlights that cost per annum estimates for a given scenario can vary quite substantially depending on input parameters, some of which are quite difficult to constrain from field observations. Therefore, practitioners should be cautious about the absolute costs estimates, especially if k is not well constrained. However, the relative rankings of the different measures remain rather consistent and, therefore, this methodology remains beneficial as a decision-support tool. We propose that this methodology can be followed by practitioners to determine which stabilisation measure results in the lowest

Table 9

Sensitivity analysis of the cost per annum (CE_n) to the number of remediation days. The cell colour scale is from dark green to yellow, where dark green is the most cost-efficient stabilisation measure (lowest CE_n) and yellow indicates the least cost-efficient stabilisation measure (highest CE_n). NPR = Nepalese Rupee.

Remediation Days	BC	RP	MW	AN
	Base case	Reprofiled	Masonry wall	Anchors
	NPR/year	NPR/year	NPR/year	NPR/year
7	2,225,473	214,737	3,275,831	145,172
14	978,144.58	202,359.24	1,464,333	110,148
30	477,310	197,167	736,309	95,616
60	256,636.86	194,964.28	416,016	89,343
90	183,147.37	194,282.48	309,158	87,391
180	111,245.10	193,705.57	205,344	85,684
270	90,557.44	193,705.57	177,484	85,614
365	79,318	193,653	162,493	85,475

cost per annum, and also how the cost per annum compares between different stabilisation measures.

4.2. Indirect costs

In this paper, the cost efficiency of different slope stabilisation measures are evaluated in terms of direct cost (initial construction, maintenance, and post-failure remediation). Indirect costs are those incurred beyond the physical damage of the slope, often due to blockage of the road (e.g. cost of traffic taking alternative, longer, routes in terms of: petrol, goods delays, and productivity loss) [2,16]. Given that the case study cut slope is on a key goods route from India to Kathmandu, delay costs caused by road closure could be very high. These indirect costs are more challenging to account for and can be incurred long after the event itself, therefore, they are often underestimated [25]. Including indirect costs in this analyses could considerably increase overall costs, for stabilisation measures where the F_f is high and landslide debris frequently blocked the road. However, it is important to note that cut slope failures do not always result in road blockage as this depends on the volume of landslide debris and thus the extent of the failure surface [14]. Although, given that this road is only one lane in each direction (around 9–11 m total width), with little extra space, even partial blockage of one lane, would likely cause considerable delay.

MacLeod et al. [25] present three methods for estimating the indirect costs of landslides: (1) unit cost estimation (e.g. road closure costs); (2) probabilistic-based assessment (suitable where there are a large range of geographically dispersed landslide impacts); and (3) survey data collection from personal accounts. The unit cost estimation for road closure would be most suitable for this case, but requires traffic flow data. Negi et al. [29] use this method to determine the cost of detouring during the closure of the National Highway 58 in Garhwal Himalaya, India, due to a landslide. They attributed 92 % of the overall cost to indirect costs and just 8 % to direct costs. However, the restoration work (which constituted 96 % of the direct costs) only included the excavation of material and not works to stabilise the slope.

Hearn et al. [16] carried out an extensive cost analysis study on landslides on the national road network of Laos. They do not include the cost of detours as they state that there are limited viable alternative routes given the sparse road network. This is also the case for many regions of Nepal. Instead, they account for the waiting times, average passenger numbers, value of time (VoT), and vehicle operating costs (VOC). VoT includes gross domestic product (GDP) per head, working age population, unemployment rates, and working hours per annum (found to be USD 0.55/hr per vehicle for Laos). VOC includes costs of vehicle hiring/purchase, driving labour costs, and fuel costs. VOC values vary based on the blockage period. Hearn et al. [16] calculate the traffic cost of road closure by multiplying overall road closure time for all

vehicles involved by USD 8.8 per hour (derived from VOC and VoT). It is assumed that if the blockage is less than 24 h, then all vehicles pass during the daylight hours (16-h period). Therefore, the overall road closure time for all vehicles involved is calculated using one of the following two equations:

If the blockage is <24 h:

$$(\text{Blockage time} \times \text{AADT})/16 \quad (4)$$

If the blockage is >24 h:

$$(\text{Blockage time} \times \text{AADT})/24 \quad (5)$$

where AADT is the annual average daily traffic.

We adopt the approach from Hearn et al. [16] to estimate the magnitude of indirect costs that would be required to change our results. The overall road closure time for all vehicles involved is determined using Eqs. 4 and 5 under different scenarios for road closure times (2, 4, 8, 12, 16, 24, 48, 72 h) and AADT = 5,963 (value of AADT for 2010 for the Narayanghat-Mugling road from Department of Roads [5]; Ojha [30]). These road closure times are chosen based on field experience in Nepal for time taken to clear roads when they are blocked (this is different to remediation times which are the times taken to remediate the slope). Given that we do not have the required information for VOC and VoT, the overall road closure times for all vehicles involved are multiplied by an arbitrary figure of USD 10 (in place of the USD 8.8 used by Hearn et al. [16]), which is equal to NPR 1273, to approximate an overall traffic cost of road closure. For each stabilisation measure, the overall traffic cost of road closure is then multiplied by the F_f and added to the direct CE_n (for the most likely parameter set given in Table 5) for each to get an overall CE_n (Table 10).

In this analysis, which accounts for indirect and direct costs using the original chosen input parameter values, for the full range of road closure times tested, AN remains the most cost-efficient stabilisation measure. However, BC replaces MW as the least cost-efficient stabilisation measure for all the road closure times tested. This analysis involves strong assumptions (no detours) and uncertain estimates (USD 10 per hour to account for VOC and VoT) but gives an indication of how indirect costs might influence the cost efficiency of the outcomes. Multiple values of AADT were tested (more than and less than 5963) to find the combinations of AADT and closure time required to alter the most and least cost-efficient scenario. RP replaces AN as most cost-efficient for AADT $\geq 20,000$ and closure times ≥ 72 h; when AADT = 1000, MW is least cost-efficient for closure times ≤ 8 h, whereas BC is least cost-efficient for road closure times ≥ 12 h.

The sensitivity analysis for the input parameters tested in Section 3.2 (99th percentile value for k , porosity, the inclination of the impermeable boundary, and the remediation time) was also applied to the cost-benefit analysis that includes direct and indirect costs under road closure times

Table 10

A table of estimated cost per annum (CE_n) including indirect costs based on overall traffic cost for road closure times of 2–72 h and the annual average daily traffic, AADT = 5963. Overall traffic cost of road closure is added to the existing CE_n from direct costs to get a new CE_n . Overall traffic cost of closure is calculated by multiplying closure times for all vehicles by USD 10. Closure times are determined using Eqs. 4 and 5. The cell colour scale is from dark green to yellow, where dark green is the most cost-efficient stabilisation measure (lowest CE_n) and yellow indicates the least cost-efficient stabilisation measure (highest CE_n). NPR = Nepalese Rupee.

	BC	RP	MW	AN
	NPR/year	NPR/year	NPR/year	NPR/year
CE_n	183,147	194,282	309,157	87,391
Closure time	New CE_n (NPR/year)			
2	623,202	194,809	582,016	89,557
4	1,063,257	195,335	854,874	91,723
8	1,943,367	196,388	1,400,589	96,054
12	2,823,477	197,440	1,946,305	100,385
16	3,703,587	198,493	2,492,021	104,717
24	3,703,587	198,493	2,492,021	104,717
48	7,224,026	202,704	4,674,884	122,042
72	10,744,466	206,914	6,857,747	139,367

of 2, 4, 8, 12, 16, 24, 48, 72 h and AADT = 5,963. The same parameter values were tested as in Section 3.2. For porosity, AN remains most cost-efficient in all cases except when road closure time is 72 h and porosity is 5 % (when RP becomes most cost-efficient); BC is least cost-efficient in all cases except road closure time is 2 h and porosity is 5 % (when MW is least cost-efficient). For remediation time, AN is most cost-efficient unless closure times are 12–72 h for 7 days remediation or 48–72 h for 14 days remediation (when RP is most cost-efficient). BC is always least cost-efficient unless closure time is 2 h for 270–365 days remediation (when MW is the least cost-efficient). When varying the 99th percentile of k , the most cost-efficient scenario is always AN, and the least is always BC. For the inclination of the impermeable boundary, AN is most cost-efficient for all closure times when the inclination is 15° and for 2–24 h closure for 20° inclination; RP is most cost-efficient for 48–72 h for 20° inclination and for all closure times for 25° inclination. BC is always the least cost-efficient with the exception of a 2-h closure time for 20° inclination and 2–8-h closure times for 25° inclination.

There is a difference between closure timescales (2–72 h) and remediation timescales (7–365 days). These reflect the difference between clearing debris from the road to the point where traffic can pass and returning the slope to its stabilised condition. This raises the question: what happens in the period after reopening and before remediation? In practice, it is possible that the slope fails again during this period but we are unable to capture this in our analysis since we only ‘count’ failures to the slope after remediation. This is appropriate for direct costs since it is only then that new direct costs are incurred but is a problem for indirect costs since disruption returns. Our current approach implicitly assumes that no failures occur between road reopening and slope remediation. Relaxing this assumption is difficult because each failure alters the cut slope geometry (which is only reconstructed during remediation). This is difficult to represent in the model and would require additional assumptions about runoff of failed material. Predicted post-failure slope geometry will be highly uncertain and this uncertainty would propagate into each subsequent stability analysis.

It is also important to note that the approaches used by Hearn et al. [16] and MacLeod et al. [25] are quite crude as they treat all vehicles as the same, masking very considerable variability in reality. Alternatively, Winter et al. [45,46] use the QUADRO (QUEues And Delays at ROad-works) model, which can assess the costs imposed on road users, including delays, accounting for vehicle type. They consider these direct consequential economic impacts (disruption to infrastructure and loss of

utility). Winter et al. [45,46] also evaluate direct (direct costs of the clean-up and remediation) and indirect consequential economic impacts (disruption to transport-dependent activities) to landslides. They incorporate the concept of the ‘vulnerability shadow’: the areal extent of the impact of closures accounting for access to opportunities (e.g. education, employment, wealth etc.).

5. Conclusions

This paper presents a novel cost-benefit analysis methodology for road cut slopes based on a mechanistic probabilistic model. The methodology can be used to compare the cost efficiency of different slope stabilisation options for a road cut slope accounting for the direct costs of: initial investment, maintenance, and remedying slope failure. The cost of remedying slope failure depends on the annual frequency of slope failure (F_f), which is estimated using the CUTSTAB-P methodology recently proposed in Robson et al. [35]. The costs are estimated using a region-specific system of rate analysis that gives standardised costing estimates for budgeting. Unlike other cost analyses for slope stability, the presented methodology accounts for uncertainty in slope geo-material characteristics, as well as for hillslope hydrology.

The methodology was demonstrated on a road cut slope in Nepal where four slope stabilisation measure scenarios were tested. The cost-benefit analysis finds that: the anchoring system would be the most cost-efficient for this cut slope (whether accounting for only direct or also indirect costs); and that the mortared masonry wall would be the least cost-efficient. Model sensitivity testing suggests that: the anchoring system remains the most cost-efficient stabilisation measure in 84 % of cases, the base case is most cost-efficient in 11 % of cases, and the reprofiled cut slope is most cost-efficient in 5 % of cases. Sensitivity testing suggests that the mortared masonry wall is the least cost-efficient in 79 % cases, with the reprofiled cut slope least efficient for the remaining 21 % of the cases. When accounting for indirect costs, the anchoring system is the most cost-efficient for 100 % of the road closure times tested. When including indirect costs, the base case becomes least cost-efficient for 100 % of the road closure times tested. Given that mortared masonry walls of the style tested here are implemented widely along roads in Nepal, we suggest that a large amount of money is being lost every year by implementing this stabilisation measure rather than longer lasting measures like anchoring systems. However, we note that anchoring systems are not necessarily the best stabilisation measure, only the best of those evaluated in this study and for this cut slope.

Declaration of competing interest

The authors declare the following financial interests/personal relationships which may be considered as potential competing interests: Ellen Robson reports financial support was provided by NERC. If there are other authors, they declare that they have no known competing financial interests or personal relationships that could have appeared to influence the work reported in this paper.

Data availability

Data will be made available on request.

Acknowledgements

This research was supported by NERC IAPETUS Doctoral Training Partnership [Grant No.: NE/S007431/1].

References

- Bloechl A, Braun B. Economic assessment of landslide risks in the Swabian Alb, Germany—research framework and first results of homeowners' and experts' surveys. *Nat Hazards Earth Syst Sci* 2005;5(3):389–96. <https://doi.org/10.5194/nhess-5-389-2005>.
- Browne D, Ryan L. Comparative analysis of evaluation techniques for transport policies. *Environ Impact Assessment Rev* 2011;31(3):226–33. <https://doi.org/10.1016/j.eiar.2010.11.001>.
- Bründl M, Romang HE, Bischof N, Rheinberger CM. The risk concept and its application in natural hazard risk management in Switzerland. *Nat Hazards Earth Syst Sci* 2009;9(3):801–13. <https://doi.org/10.5194/nhess-9-801-2009>.
- Department of Roads. *Roadside Geotechnical Problems: A practical guide to their solution*. Government of Nepal, Ministry of Physical Planning and Works, Kathmandu; 2007.
- Department of Roads. *Design Report of Narayanghat-Mugling Road 2010 AD*. RSDP, Nepal; 2010.
- Department of Roads. *Road network data*, Government of Nepal, Ministry of Physical Infrastructure and Transport; 2017.
- Elster J. *Ulysses and the sirens: studies in rationality and irrationality*. Cambridge: Cambridge University Press; 1979.
- Fenton GA, Griffiths DV. *Risk assessment in geotechnical engineering*. John Wiley & Sons, Inc.; 2008. <https://doi.org/10.1002/9780470284704>.
- Fine. Unit weight of Rocks; 2023. URL: <https://www.finesoftware.eu/help/geo5/en/unit-weight-of-rocks-01/>.
- Froude MJ, Petley DN. Global fatal landslide occurrence from 2004 to 2016. *Nat Hazards Earth Syst Sci* 2018;18:2161–81. <https://doi.org/10.5194/nhess-18-2161-2018>.
- Glewwe P, Todd P. Cost-benefit analysis and cost-effectiveness analysis. *Impact evaluation in international development: theory, methods, and practice*. World Bank Publications; 2022. <https://doi.org/10.1596/978-1-4648-1497-6>.
- Grima N, Edwards D, Edwards F, Petley D, Fisher B. Landslides in the andes: forests can provide cost-effective landslide regulation services. *Sci Total Environ* 2020; 745. <https://doi.org/10.1016/j.scitotenv.2020.141128>.
- Gwilliam K. *Transportation project appraisal at the World Bank*. ECMT-OECD Seminar on Evaluation Methodologies for Infrastructure Investments and Urban Sprawl. Paris; 2000.
- Hearn GJ. *Slope engineering for mountain roads*, Geological Society Engineering Geology Special Publication no. 24, Geological Society of London; 2011.
- Hearn GJ, Hunt T, Aubert J, Howell J, Chigira M. *Landslide impacts on the road network of Lao PDR and the feasibility of implementing a slope management programme*. In: *International Conference on Management of Landslide Hazard in the Asia-Pacific Region*, Sendai, Japan; 2008.
- Hearn GJ, Kerridge MSP, Pongpanya P. Landslide costs on the national road network of Laos, with some regional implications. *Q J Eng Geol Hydrogeol* 2021;54(4). <https://doi.org/10.1144/qjgeh2021-023>.
- Hearn GJ, Pongpanya P. Developing a landslide vulnerability assessment for the national road network in Laos. *Q J Eng Geol Hydrogeol* 2020;5(3). <https://doi.org/10.1144/qjgeh2020-110>.
- Hearn GJ, Shakya NM. Engineering challenges for sustainable road access in the Himalayas. *Q J Eng Geol Hydrogeol* 2008;50(1):69–80. <https://doi.org/10.1144/qjgeh2016-109>.
- Holcombe E, Smith S, Wright E, Anderson MG. An integrated approach for evaluating the effectiveness of landslide risk reduction in unplanned communities in the Caribbean. *Nat Hazards* 2012;61(2):351–85. <https://doi.org/10.1007/s11069-011-9920-7>.
- Klose M, Danm B, Terhorst B. Landslide cost modeling for transportation infrastructures: a methodological approach. *Landslides* 2015;12:321–34. <https://doi.org/10.1007/s10346-014-0481-1>.
- Kull D, Mechler R, Hochrainer-Stigler S. Probabilistic cost-benefit analysis of disaster risk management in a development context. *Disasters* 2013;37(3):374–400. <https://doi.org/10.1111/disa.12002>.
- Lennartz T. Constructing roads—constructing risks? Settlement decisions in view of landslide risk and economic opportunities in Western Nepal. *Mountain Res Develop* 2013;37(4):364–71. URL: <https://www.jstor.org/stable/mounresedev.33.4.364>.
- Li AJ, Cassidy MJ, Wang Y, Merifield RS, Lyamin AV. Parametric Monte Carlo studies of rock slopes based on the Hoek-Brown failure criterion. *Comput Geotech* 2012;45:11–8. <https://doi.org/10.1016/j.compgeo.2012.05.010>.
- Marinos P, Hoek E. GSI: a geologically friendly tool for rock mass strength estimation. *ISRM International Symposium*; 2000.
- MacLeod A, Hofmeister RJ, Wang Y, Burns S. *Landslide indirect losses: methods and case studies from Oregon*. Open File Report O-05-X. Oregon Department of Geology and Mineral Industries; 2015.
- McAdoo BG, Quak M, Gnyawali KR, Adhikari BR, Devkota S, Rajbhandari PL, Sudmeier-Rieux K. Roads and landslides in Nepal: how development affects environmental risk. *Nat Hazards Earth Syst Sci* 2018;18(12):3202–10. <https://doi.org/10.5194/nhess-18-3203-2018>.
- National Planning Commission. *Status and Roadmap: 2016–2030*. Government of Nepal; 2017.
- National Research Council. *Partnerships for reducing landslide risk: assessment of the national landslide hazards mitigation strategy*. National Academies Press; 2004.
- Negi IS, Kumar K, Kathait A, Prasad PS. Cost assessment of losses due to recent reactivation of Kaliasaur landslide on National Highway 58 in Garhwal Himalaya. *Nat Hazards* 2015;68(2):901–14.
- Ojha KN. Overloading and pavement service life—a case study on Narayanghat-Mugling road, Nepal. *J Transp Technol* 2010;8(4):343–56. <https://doi.org/10.4236/jtts.2018.84019>.
- Rural Access Programme (RAP) Phase 3. *Trimester Report*; 2016.
- Reid JM, Clark GT. A whole life cost model for earthworks slopes, Transport Research Laboratory, TRL Report 430; 2000.
- Robson E, Utili S, Milledge D. Road slope stabilisation in Nepal: stakeholder perspectives. *SCG-XIII International Symposium on Landslides*, Cartagena. 2020. URL: <https://www.issmge.org/publications/publication/road-slope-stabilisation-in-nepal-stakeholder-perspectives>.
- Robson E, Agosti A, Utili S, Milledge D. A methodology for road cutting design guidelines based on field observations. *Eng Geol* 2022;307. <https://doi.org/10.1016/j.enggeo.2022.106771>.
- Robson EB, Milledge D, Utili S, Dattola G. Probability of rainfall triggered slope failure estimated via hillslope hydrogeological modelling and probabilistic stability analyses. *Rock Mech Rock Eng* 2023. <https://doi.org/10.1007/s00603-023-03694-5>.
- Salbego G, Floris M, Busnardo E, Toaldo M, Genevois R. Detailed and large-scale cost/benefit analyses of landslide prevention vs. post-event actions. *Nat Hazards Earth Syst Sci* 2015;15(11):2461–72. <https://doi.org/10.5194/nhess-15-2461-2015>.
- Sana E, Kumar A, Robson E, Prasanna R, Kala U, Toll DG. Preliminary assessment of series of landslides and related damage by heavy rainfall in Himachal Pradesh, India, during July 2023. *Landslides* 2024. <https://doi.org/10.1007/s10346-023-02209-1>.
- Shakya NM, Nirula DR. Integration of bio-engineering techniques in slope stabilisation works: a cost-effective approach for developing countries, First World Landslide Forum, International Consortium on Landslides, United Nations University, Japanese Landslide Society, Tokyo; 2008.
- Singhal BB, Gupta RP. *Applied hydrogeology of fractured rocks*. 2nd ed. Springer Science+Business; 2010.
- St. Clair J, Moon S, Holbrook WS, Perron JT, Riebe CS, Martel SJ, Carr B, Harman C, Singha K, deB Richter D. Geophysical imaging reveals topographic stress control of bedrock weathering. *Science* 2015;350(6260). <https://doi.org/10.1126/science.aab221>.
- Troch PA, Paniconi C, Emiel van Loon E. Hillslope-storage Boussinesq model for subsurface flow and variable source areas along complex hillslopes: 1. Formulation and characteristic response. *Water Resour Res* 2003;20(11). <https://doi.org/10.1029/2002WR001728>.
- United Nations. Sustainable Development Goal 9: SDG indicator 9.1.1; 2007. URL: <https://sdg-tracker.org/infrastructure-industrialization>.
- Vagdatli T, Petrousatou K. Modelling approaches of life cycle cost–benefit analysis of road infrastructure: a critical review and future directions. 2000;13(1). <https://doi.org/10.3390/buildings13010094>.
- Australian Geomechanics Society. *Practice Note Guidelines for Landslide Risk Management* 2007. *Austr Geomech J News Austr Geomech Soc* 2007;42(1).
- Winter MG, Shearer B, Palmer D, Peeling D, Peeling J, Harmer C, Sharpe J. *Assessment of the economic impacts of landslides and other climate-driven events*. *Transp Res Lab* 2018.
- Winter MG, Shearer B, Palmer D, Peeling D. Economic impacts of landslides and floods on a road network. *Geographica* 2019;54(2):207–20. <https://doi.org/10.1016/j.proeng.2016.06.168>.
- Wong HN, Ho KK, Chan YC. *Assessment of consequences of landslides*. In: *Proceedings of the International workshop on landslide risk assessment*; 1997. p. 111–49.